Chin. Ann. Math. Ser. B
43(6), 2022, 1033–1048
DOI: 10.1007/s11401-022-0376-8

Chinese Annals of
Mathematics, Series B

Recent Progress in Applications of the Conditional Nonlinear Optimal Perturbation Approach to Atmosphere-Ocean Sciences*

Mu MU[1] Kun ZHANG[2] Qiang WANG[3]

Abstract The conditional nonlinear optimal perturbation (CNOP for short) approach is a powerful tool for predictability and targeted observation studies in atmosphere-ocean sciences. By fully considering nonlinearity under appropriate physical constraints, the CNOP approach can reveal the optimal perturbations of initial conditions, boundary conditions, model parameters, and model tendencies that cause the largest simulation or prediction uncertainties. This paper reviews the progress of applying the CNOP approach to atmosphere-ocean sciences during the past five years. Following an introduction of the CNOP approach, the algorithm developments for solving the CNOP are discussed. Then, recent CNOP applications, including predictability studies of some high-impact ocean-atmospheric environmental events, ensemble forecast, parameter sensitivity analysis, uncertainty estimation caused by errors of model tendency or boundary condition, are reviewed. Finally, a summary and discussion on future applications and challenges of the CNOP approach are presented.

Keywords Conditional nonlinear optimal perturbation, Atmosphere, Ocean, Targeted observation, Predictability
2000 MR Subject Classification 17B40, 17B50

1 Introduction

Spatial-temporal evolutions of atmospheric and oceanic motions are governed by a group of nonlinear partial differential equations. These nonlinear equations are established on the Navier-Stokes equations in the frame of Geophysical Fluid Dynamics (see [1–2]). Regarding specific issues, various equations are obtained via scale analysis and other simplification, such as quasi-geostrophic approximation, β-plane approximation, etc. Numerical models are exe-

Manuscript received March 25, 2022. Revised June 23, 2022.
[1]Department of Atmospheric and Oceanic Sciences and Institute of Atmospheric Sciences, Fudan University, Shanghai 200438, China; CMA-FDU Joint Laboratory of Marine Meteorology, Shanghai 200438, China; Shanghai Frontiers Science Center of Atmosphere-Ocean Interaction, Shanghai 200438, China. E-mail: mumu@fudan.edu.cn
[2]CAS Key Laboratory of Ocean Circulation and Waves, Institute of Oceanology, Chinese Academy of Sciences and Qingdao National Laboratory for Marine Science and Technology, Qingdao 266071, China. E-mail: kzhang@qdio.ac.cn
[3]Key Laboratory of Marine Hazards Forecasting, Ministry of Natural Resources, Hohai University, Nanjing 210098, China; College of Oceanography, Hohai University, Nanjing 210098, China. E-mail: wangq@hhu.edu.cn
*This work was supported by the National Natural Science Foundation of China (Nos. 41790475, 92158202, 42076017, 41576015) and Guangdong Major Project of Basic and Applied Basic Research (No. 2020B0301030004).

cutable codes obtained by discretizing the above analytical equations, which can quantitatively simulate the states, motions, and dynamical processes of the focused phenomena. Since the first atmospheric model in the early 1950s (see [3]) and the first oceanic model in the late 1960s (see [4]), numerical models have been widely utilized and currently play a critical role in the atmospheric-oceanic sciences (see [5]). On one hand, meteorological and oceanic forecasts now greatly rely on numerical modeling. On the other hand, model data, as complementary to observational data, have comprehensively deepened the understanding of the motions in the atmospheric and oceanic fluids.

In general, to perform simulations or predictions with numerical models, initial and boundary conditions are necessary, as well as appropriate values of model parameters that correspond to parameterizations of various physical processes (e.g., bottom drag, vertical mixing). However, true states of initial and boundary conditions can never be acquired due to inadequate observations and measurement errors. Besides, inaccuracies also commonly exist in model parameters. Owing to uncertainties of initial conditions, boundary conditions and model parameters, numerical simulations or predictions inevitably exist uncertainties (see [6–7]). Predictability study aims to reveal the sources causing the uncertainties of model results, uncover the related mechanisms, and further seek potential ways to reduce these uncertainties (see [8–9]). It is a fundamental issue in atmosphere-ocean sciences. With more and more concerns on predicting weather, ocean and climate, atmospheric and oceanic predictability studies have achieved significant progress during the past several decades (see [10–12]).

Since the first investigation in atmospheric predictability conducted by Thompson [13], several methods, like the ensemble approach (see [14]), predictive power (see [15]), and singular vector (SV for short) (see [16]), have been utilized in atmospheric and oceanic predictability studies. Among them, the SVs that represent the optimal perturbations showing the largest transient growth in linear frameworks have been widely used (see [17]). For instance, the impacts of initial perturbations on atmospheric motions were examined with the SV method by Lorenz [18] and Farrell [19]. By combining the SV with oceanic general circulation models, [20] and [21] explored the predictabilities of the Kuroshio large meander formation and the Atlantic meridional overturning circulation, respectively. Notably, the SV approach is only applicable to the systems that linear approximation holds. Since most atmospheric and oceanic models are nonlinear ones, to apply the SV approach, the perturbations need to be small enough and the corresponding tangent linear model should be capable of simulating the temporal evolutions of the perturbations. It is clear that these conditions limit the ability of the SV approach to investigate nonlinear physical processes, especially when nonlinearity has remarkable effects on simulating or forecasting ocean-atmospheric motions (see [22–23]).

Regarding this, Mu et al. [24] proposed an innovative approach to investigate the optimal initial perturbation that causes the largest perturbation growth at a future time under a given physical constraint. This approach fully considers nonlinearity without any linear approximation and is named the conditional nonlinear optimal perturbation (CNOP for short). Seven years later, when investigating the transition from laminar to turbulent states in fluid mechanics, an optimal initial perturbation method that is the same as the CNOP presented in [24] is reported (see [25–26]). According to its physical meaning, the CNOP can not only help to identify the optimal precursor (OPR for short) of an anomalous atmospheric or oceanic event and uncover the triggering mechanism, but also reveal the optimally growing initial error (OGIE for short) related to the forecast of the concerned event. Moreover, the spatial distribution of the CNOP can be used to determine sensitive areas for targeted observation (see [27–28]). The C-NOP was first proposed to deal with initial perturbations (denoted as CNOP-I hereinafter) (see [24]). During the past decade, to consider the other aspects causing prediction uncertainties, we have extended the CNOP approach to deal with perturbations of model parameters (CNOP-P) (see [29]), model tendency or forcing (nonlinear forcing singular vector, i.e., NFSV, also named CNOP-F) (see [30]) and boundary conditions (CNOP-B) (see [31]). A detailed mathematical description of the extended CNOP approach is presented in Section 2.

To date, the CNOP approach has been widely applied to explore the predictabilities of high-impact ocean-atmospheric environmental events. In detail, the CNOP-I approach has been used to address the predictabilities of the thermohaline circulation in the ocean (see [32–33]), the El Niño Southern Oscillation (ENSO for short) (see [34–38]), the double-gyre ocean circulation (see [39]), blocking (see [40–41]), tropical cyclone (see [42]), variations of the Kuroshio (see [22, 43–44]), etc. Simultaneously, the CNOP-I has been utilized in determining sensitive areas of targeted observations (see [45–47]) and generating initial perturbations for ensemble prediction (see [48–50]). Moreover, the extended CNOP approaches are attracting more and more attention. For instance, the CNOP-P was successfully employed to examine parameter sensitivities in both land models (see [51–53]) and ocean ecosystem models (see [54]). The CNOP-F was employed to identify the most disturbing tendency error for El Niño predictions in the Zebiak–Cane (ZC for short) model (see [55]).

The CNOP applications before 2016 have been reviewed in several papers (see [12, 56]). This paper primarily reviews the CNOP-related works during the past five years, which is arranged as follows: Section 2 presents a description of the CNOP approach. Section 3 addresses the algorithm developments for solving CNOP. Section 4 highlights the progress of applying the CNOP in atmosphere-ocean sciences, including the recent applications of CNOP-I, CNOP-P, CNOP-F and CNOP-B, respectively. Finally, a summary and discussion are given in Section 5.

2 Theoretical Frameworks of the CNOP Approach

Following [57], this section will describe the CNOP approach in a uniform form, including CNOP-I, CNOP-P, CNOP-F and CNOP-B. A numerical model can be written as follows:

$$\begin{cases} \dfrac{\partial \mathbf{U}(\mathbf{x},t)}{\partial t} = F(\mathbf{U}(\mathbf{x},t), \mathbf{P}(t)), \\ \mathbf{U}(\mathbf{x},t)|_{t=0} = \mathbf{U}_0(\mathbf{x}), \\ B(\mathbf{U}(\mathbf{x},t))|_{\Gamma} = \mathbf{G}(\mathbf{x},t), \end{cases} \tag{2.1}$$

where $\mathbf{U}(\mathbf{x},t)$ is the state vector in the model with $\mathbf{U}_0(\mathbf{x})$ representing the initial condition, and t is the time with $t=0$ representing the initial time. $\mathbf{x}\in\Omega$ is the spatial variable, where Ω denotes the model domain. F is the nonlinear partial differential operator and $\mathbf{P}(t)$ is the parameter vector. B is the boundary condition operator with Γ denoting the boundary of Ω and $\mathbf{G}(\mathbf{x},t)$ is the time-varying boundary condition.

Supposing $\mathbf{u}_0(\mathbf{x})$, $\mathbf{g}(\mathbf{x},t)$, $\mathbf{p}(t)$ and $\mathbf{f}(\mathbf{x},t)$ are the perturbations of initial conditions, boundary conditions, model parameters and model tendencies, respectively, (2.1) then is changed as:

$$\begin{cases}\dfrac{\partial(\mathbf{U}(\mathbf{x},t)+\mathbf{u}(\mathbf{x},t))}{\partial t}=F(\mathbf{U}(\mathbf{x},t)+\mathbf{u}(\mathbf{x},t),\mathbf{P}(t)+\mathbf{p}(t))+\mathbf{f}(\mathbf{x},t),\\ (\mathbf{U}(\mathbf{x},t)+\mathbf{u}(\mathbf{x},t))|_{t=0}=\mathbf{U}_0(\mathbf{x})+\mathbf{u}_0(\mathbf{x}),\\ B(\mathbf{U}(\mathbf{x},t)+\mathbf{u}(\mathbf{x},t))|_{\Gamma}=\mathbf{G}(\mathbf{x},t)+\mathbf{g}(\mathbf{x},t),\end{cases}\tag{2.2}$$

where $\mathbf{u}(\mathbf{x},t)$ denotes the state vector change caused by the perturbations. To estimate the maximal impact of the perturbations, a constrained optimization problem is established:

$$J(\mathbf{u}_{0\delta}(\mathbf{x}),\mathbf{p}_{\varepsilon}(t),\mathbf{f}_{\gamma}(\mathbf{x},t),\mathbf{g}_{\sigma}(\mathbf{x},t))=\max J(\mathbf{u}(\mathbf{x},\tau)),\tag{2.3}$$

where J is the cost function that evaluates the evolution of $\mathbf{u}(\mathbf{x})$ at a forecast time τ. Various perturbations are limited by the constraint conditions of $\mathbf{u}_0(\mathbf{x})\in C_\delta,\mathbf{p}(t)\in C_\varepsilon,\mathbf{f}(\mathbf{x},t)\in C_\gamma$ and $\mathbf{g}(\mathbf{x},t)\in C_\sigma$, where $C_\delta,C_\varepsilon,C_\varepsilon$ and C_γ are determined by physical considerations.

The solution of (2.3), referring to the optimal combination mode of $\mathbf{u}_{0\delta}(\mathbf{x}),\mathbf{p}_{\varepsilon}(t)$,$\mathbf{f}_{\gamma}(\mathbf{x},t)$ and $\mathbf{g}_{\sigma}(\mathbf{x},t)$ is called the CNOP. If only the initial condition perturbation is considered, the solution of (2.3) is CNOP-I. Similarly, we can also obtain CNOP-P, CNOP-F or CNOP-B by only considering the perturbations of model parameters, model tendency or boundary condition, respectively.

3 Recent Algorithm Developments for Solving CNOPs

Determining the increasing direction of the cost function is one critical step to solve the optimization problem in (2.3). One common way to obtain this direction is through the gradient of the cost function to variables by integrating adjoint models (see [39, 47]). However, the adjoint models of many models have not been implemented yet. Under such circumstances, adjoint-free methods, including the gradient definition-based method (see [58]), ensemble methods (see [59–60]), and intelligent optimization methods (see [61–62]), were developed to calculate CNOPs.

In earlier times, the adjoint-free methods were primarily utilized in simple models with small optimization dimensions, which are usually less than $\mathbf{O}(10^3)$. One main reason is that the adjoint-free methodology requires a great number of nonlinear model integrations. When the optimization dimension becomes large, the repeated nonlinear model integrations limit the calculation efficiencies of these methods. To solve this, a methodology combining dimension-reduction techniques with adjoint-free methods has been proposed.

[63] first combined the dimension-reduction approach of singular vector decomposition (SVD for short) and the ensemble technique to compute the CNOP in the ZC model. Subsequently, the CNOPs for double-gyre regime transitions modeled by the Regional Ocean Modeling System (ROMS for short) were obtained via the principal component analysis (PCA for short) dimension-reduction and the intelligent optimization method of simulated annealing (see [64]). The CNOPs for typhoons simulated by the Fifth-Generation Mesoscale Model (MM5 for short) model and ENSO Events simulated by an intermediate coupled model (ICM for short) were successfully calculated by combining dimension reduction of the PCA-based or SVD-based with gradient definition approaches (see [65–66]). It is worth mentioning that the optimal solutions obtained in these studies were acceptable and similar to those obtained by the adjoint methods.

Table 1 Summary of the algorithms for solving CNOPs that combine dimension-reduction techniques with the adjoint-free optimization methods.

Model	Optimization algorithm	Optimization dimension	Optimization dimension after post-treatment)	Reference
ZC model	SVD − basedensemble projectionalgorithm	1080	10-100	[63]
ICM model	SVD − basedgradient definitionalgorithm	8174	48	[66]
ROMS	PCA − basedsimulated annealingalgorithm	54667	70	[64]
MM5	PCA − basedgradient definitionalgorithm	202675	60	[65]
CAM4	REOF − basedparticle swarmalgorithm	64800	20	[67]
GFDL CM2p1	PCA − basedparticle swarmalgorithm	289800	330	[68]

One encouraging benefit of using the dimension-reduction technique in adjoint-free optimization approaches is the improved capability to calculate CNOPs with higher optimization dimensions. As listed in Table 1, with the help of the dimension-reduction technique, the optimized dimensions have improved from 1080 in the ZC model to 54667 in the ROMS. Recently, using the rotated empirical orthogonal function (REOF for short)-based particle swarm optimization algorithm, the CNOP-B is calculated in the atmosphere model of Community Atmosphere Model, version 4 (CAM4 for short) to identify the optimally growing boundary errors (OGBE for short) in the extended-range prediction of strong and long-lasting Ural blocking (UB for short) events (see [67]). In this study, the optimization dimension is reduced from 64800 to 20. Besides, the optimal precursor of El Niño was investigated in the coupled model of GFDL CM2p1 (see [68]), of which the optimization dimension was reduced from 289800 to 330. With increased computing power and more efficient adjoint-free optimization methods, the dimension-reduction technique will be a promising way to solve the CNOP computation in operational models without adjoint components.

4 Recent Progresses in Applications of the CNOP Approach

4.1 Progress in applications of CNOP-I

The CNOP-I represents the most unstable nonlinear non-normal mode in initial conditions. Recent applications of the CNOP-I focus on estimating the largest prediction uncertainties caused by OGIEs, and further improving prediction skills by determining sensitive areas for targeted observations.

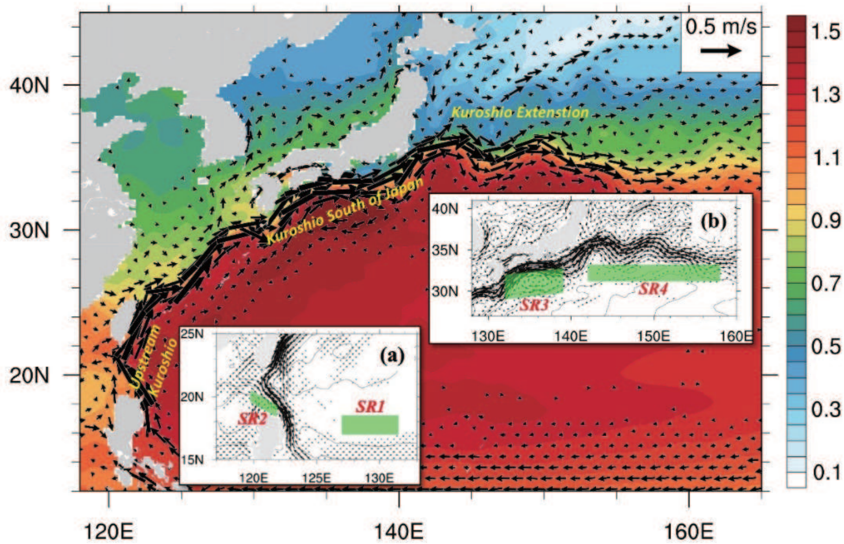

Figure 1 Sensitive areas determined by the CNOP-Is in targeted observations for predicting the seasonal transport reduction of the upstream Kuroshio (SR1), the Kuroshio intrusion into the South China Sea (SR2), the formation of the Kuroshio large meander (SR3), and the decadal state transition of the Kuroshio Extension (SR4). The shaded color and vectors represent mean absolute dynamic topography (unit: meters) and geostrophic flow derived from AVISO. The figure is from [73]. However, as OSSEs treat model outputs as pseudo' observations, no realistic in-field observations were conducted. To realistically test the impacts of the CNOP-I based targeted observations, observing system experiments (OSEs for short), which assimilate real observations in sensitive areas, are thereby needed.

In the ocean, our group has employed the CNOP-I approach to investigate the predictabilities and improve the corresponding predictions of some phenomena in the Kuroshio current, including the seasonal transport reduction of the upstream Kuroshio (see [69]), the Kuroshio intrusion into the South China Sea (see [70]), the formation of the Kuroshio large meander (see [71]), and the decadal state transition of the Kuroshio Extension (see [23]). Using both simple and operational models, the impacts of initial errors on predicting these phenomena were first studied. Then, as depicted in Figure 1, the sensitive areas were identified in targeted observation studies for predicting these anomalous events. Observing system simulation experiments (OSSEs for short), which use model outputs as the synthetic or pseudo' observations, were conducted to validate the sensitive areas determined by the CNOP-Is. The results of OSSEs indicate that reducing or eliminating initial errors in these sensitive areas can lead to prominent prediction improvements of 22.0% to 51.0%. In fact, we care about not only the Kuroshio but also other strong currents. For instance, the OPR triggering dramatic transport fluctuations of the Antarctic circumpolar current transport is investigated in 2021 (see [72]).

Regarding this, [74] determined the sensitive area for improving the thermal structure predictions in the Yellow Sea. As shown in Figure 2(a), the sensitive area is located to the northwest of the verification area, and three time-varying Z-type stations were designed in this region (Figure 2(b)). At the same time, for comparison, three mirrored observation networks were built in the verification area. The effectiveness of the CNOP-identified sensitive area was validated through a field campaign in the summer of 2019. As shown in Figure 2(c)–(g), at the prediction time, assimilating in-field observational data in the sensitive area always exhibit the best performance. This study first highlights the feasibility and effectiveness of the field-deployed targeted observation guided by the CNOP-I to decrease forecast uncertainty of oceanic motions.

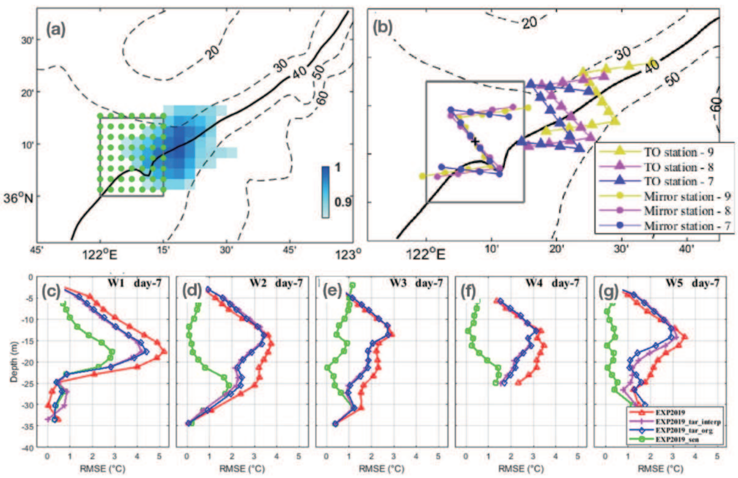

Figure 2 (a) Sensitive area (blue color) and Verification area (dotted region); (b) targeted observation stations (triangles) with mirror stations inside the verification region (circles); (c)–(g) RMSEs of temperature profiles at the prediction time (day 7), where W1–W5 refers five buoys in the verification area. Red lines are the results from the experiment without data assimilation, whereas the purple and green lines are the results of assimilating observations in the verification area and the sensitive area, respectively. The figure is reproduced from [74].

In the atmosphere, the CNOP-I approach has long been used in predictability and targeted observation studies of ENSO, typhoon, north Atlantic oscillation, etc. During the past five years, on one hand, continuous efforts have been paid in these fields and a series of achievements have

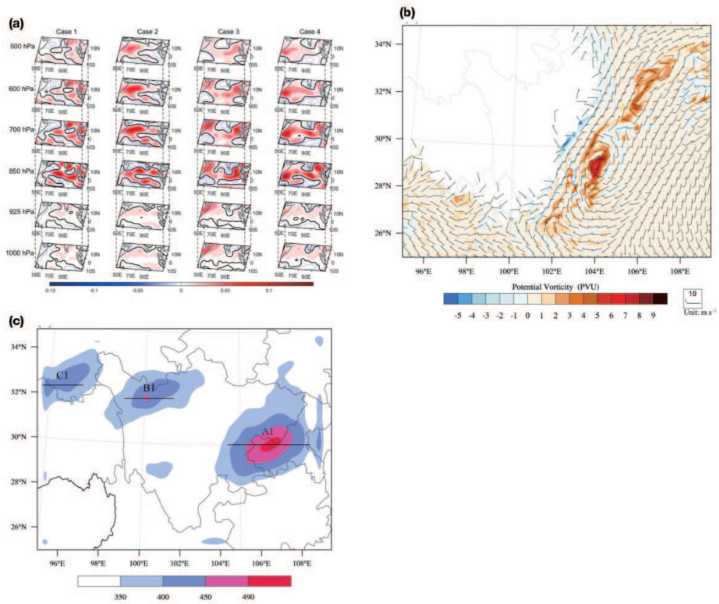

Figure 3 (a) CNOP-Is for triggering primary MJO events, adapted from [78]; (b) the simulated SWV, with color shading and vectors representing potential vorticity and wind fields (unit: ms^{-1}) at 700 hPa; (c) the sensitive areas determined by CNOP-I. Note Figures (b) and (c) are reproduced from [79].

been obtained. For instance, the CNOP-Is are further used to explore the optimal precursors and initial errors of El Niño events in operational coupled models (see [68, 75]). Simultaneously, targeted observations and ensemble forecasts of ENSO also make remarkable progress (see [76–77]).

On the other hand, researchers seek to apply the CNOP-I to deal with new scientific problems. For example, the optimal perturbations of moisture that trigger primary Madden-Julian Oscillation (MJO for short) events were first explored (see [78]). Compared to the eastern Indian Ocean, the CNOP-Is show stronger signals in the western one (see Figure 3(a)), which can trigger the MJO with a lead time of more than 15 days. Moreover, as southwest vortices (SWVs for short) in China could cause heavy rainfall and even floods, [79] used the CNOP-I to identify sensitive areas for a typical non-moving SWV (see Figure 3(b)). Figure 3(c) indicates that three sensitive areas were determined, with two located on the Eastern Tibetan Plateau and the third in the Eastern Sichuan Basin near the SWV center. Further adding observations in the sensitive areas can benefit the forecasts of SWVs.

4.2 Progress in applications of CNOP-P

In addition to uncertainties of initial conditions, model errors also severely affect the inaccuracies of numerical prediction. One primary source of model errors arises from the uncertainties of model parameters. In models, some parameters cannot be determined by observations, such as the parameters related to the stability of numerical schemes. However, some other parameters can be better determined by direct or indirect observations. In most numerical models, the number of such parameters is quite large. The CNOP-P approach is a powerful tool to estimate the sensitivity or importance of different parameters, which further guides on how to effectively improve forecast skills via observations of critical parameters. So far, the CNOP-P approach has been employed to analyze the parameter sensitivities in land models (see [80–81]) and an oceanic ecosystem model (see [54]). Since conducting additional observation for sensitive parameters is more possible to improve forecast skills, targeted observation studies of model parameters are also investigated by using the CNOP-P approach (see [82]).

Besides, new possible applications of the CNOP-P approach are being explored. By using a convection-allowing ensemble prediction system (CAEPS for short), the CNOP-P approach is innovatively used in ensemble prediction of strong convective events in South China (see [83]). In their study, to design a more reasonable formulation of model uncertainty, the most sensitive parameters that result in the largest prediction errors were first detected. Subsequently, a new formulation of model uncertainty was built by superimposing random perturbations on these sensitive parameters. Compared to the well-utilized Stochastic Perturbed Parameterization Tendencies (SPPT for short) scheme, the CNOP-P based method can potentially improve the under-dispersive problem of current CAEPSs, which brings larger spreads of humidity and temperature over the troposphere (Figure 4). As a result, the CNOP-P based method tends to cause better forecasting skills of 2-m temperature, 2-m specific humidity and hourly precipitation.

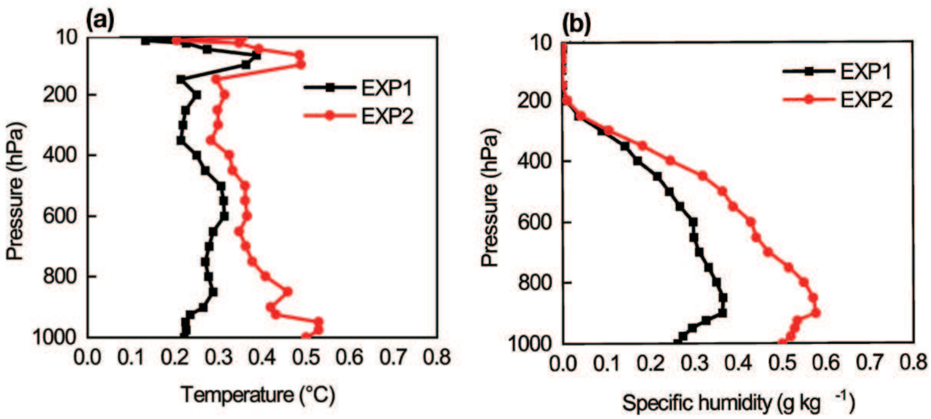

Figure 4 Vertical profiles of ensemble spread for the 24-h forecasts of 13 cases: (a) Temperature and (b) specific humidity. EXP1 and EXP2 refer to the ensemble forecasts using the SPPT scheme and the CNOP-P approach, respectively. The figure is reproduced from [83].

4.3 Progress in applications of CNOP-F

The CNOP-F seeks the optimal tendency perturbation that describes the largest combined effect of model errors (see [30]). This approach was used to investigate the prediction of El Niño and its "spring predictability barrier" (see [55, 84]). Lately, a new application of CNOP-F was proposed to reduce model errors and further improve forecasts of El Niño (see [85–86]). To date, most models cannot well simulate the occurrence and evolution of the CP-El Niño. Following this direction, an ENSO forecast system named NFSV-ICM by combining an intermediate-complexity ENSO model with the NFSV-based perturbation forecast model was established (see [86]). When this system was employed to forecast the El Niño after the mid-1970s, it well captures the distribution of sea surface temperature anomalies of the two types of El Niño (EP- and CP- Niño) events during their mature phases, although the original ICM hardly predicts the CP- Niño events. This reveals the potential application of the NFSV to data assimilation for climate prediction.

4.4 Progress in applications of CNOP-B

Uncertainties in boundary conditions also inevitably have impacts on the accuracy of numerical simulation and prediction. Exploring the uncertainties caused by boundary conditions is very important. So far, there are few predictability studies related to boundary conditions compared to predictability studies of initial conditions and model parameters. One reason is the lack of feasible methods. The CNOP-B is one useful method that can be used to conduct such studies.

By using a one-dimensional with the optimization dimension less than $O(10^3)$, the CNOP-B is first used to access the effects of boundary condition uncertainties on modeling the deep chlorophyll maximum (see [31]). Subsequently, the CNOP-B was used in a complex atmosphere model. In detail, using the CAM4 model, the CNOP-B method is utilized to investigate the impacts of Arctic sea ice concentration on extended-range prediction of strong and long-lasting UB events in winter (see [67]). The UB events are usually followed by amplification of the Siberian High (see [87]) and subsequent outbreaks of cold air in East Asia during the winter (see [88]). The UB frequency has shown an increasing trend in recent decades, which may be affected by sea ice changes in the Arctic (see [89]). Boundary conditions like Arctic sea ice may play an important role in the UB formation. The Arctic sea ice concentration (SIC for short) is crucial for extended-range prediction of strong and long-lasting UB formation.

By applying the REOF-based particle swarm optimization algorithm, the conditional nonlinear optimal perturbation is calculated to identify the OGBE in the extended-range prediction of strong and long-lasting UB formation. It is noted that SIC perturbations in the Greenland Sea (GS for short), Barents Sea (BS for short) and Okhotsk Sea (OKS for short) are important for strong and long-lasting UB formation prediction in four pentads. Moreover, the SIC per-

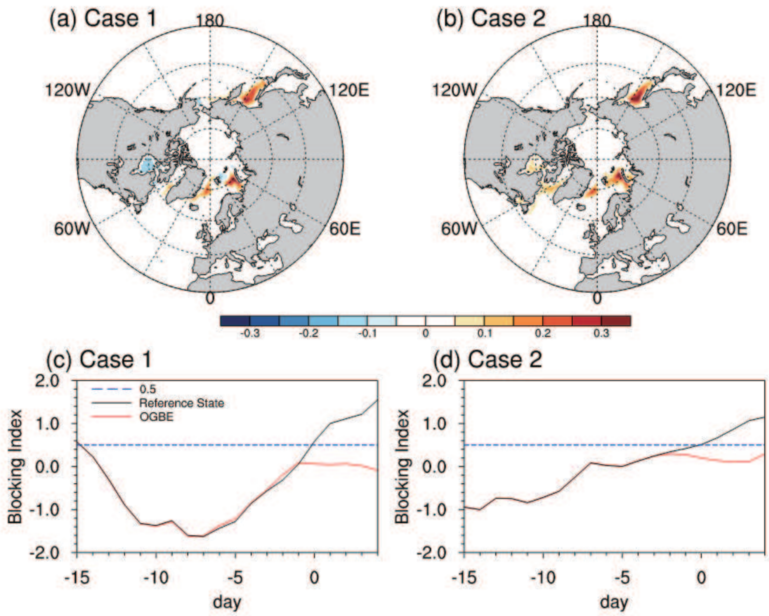

Figure 5 (a)–(b) OGBEs in two cases and (c)–(d) corresponding evolutions of UB index changes caused by the OGBEs. The figure is reproduced from [67].

turbations are mainly positive, which causes the UB events to be weakened (see Figure 5). The local characteristics of the SIC perturbations indicate that the GS, BS and OKS may be sensitive areas regarding the extended-range prediction of strong and long-lasting UB formation, which can provide scientific support for the SIC target observations in the future.

5 Summary and Discussion

Mathematically, the CNOP is the solution to a nonlinear optimization problem with an appropriate physical constraint. In essence, The CNOP-type perturbation refers to the most unstable non-normal mode, which causes the largest simulation or prediction uncertainties within a finite period and an appropriate constraint. Compared to linear approaches, the CNOP approach can well reveal the impacts of nonlinear processes, which cannot be ignored in high-impact ocean-atmospheric environmental events. The CNOP approach was first proposed to deal with uncertainties caused by initial perturbations (CNOP-I) and now has been extended to investigate the impacts of perturbations of model parameters (CNOP-P), model tendencies (CNOP-F) and boundary conditions (CNOP-B).

In this paper, the full theoretical framework of the CNOP approach is described. Subsequently, recent applications of the CNOP approach to motions of atmosphere and ocean fluids during the past five years are reviewed. Regarding the CNOP calculation, the algorithms combining dimension-reduction techniques with adjoint-free optimization techniques are becoming more and more popular. By reducing optimization dimensions, this methodology allows solving the CNOP in those complex models without adjoint models.

Regarding the CNOP applications, on one hand, the CNOP-I and the CNOP-P have been continuously employed to explore the effects of uncertainties in initial conditions and model parameters. Moreover, the CNOP-based targeted observation studies for both initial and model errors are attracting increasing attention. Notably, field-deployed targeted observations guided by the CNOP have been carried out, which show remarkable superiority compared to conventional observations. On the other hand, the CNOP approach is innovatively used in new fields, such as the pioneering use of the CNOP-P for ensemble forecasts and the CNOP-F for improving climate prediction. Besides, the CNOP-B approach, which is relatively new, is first employed in an operational atmospheric model to reveal the impacts of Arctic sea ice concentration on forecasting UB events.

So far, although the CNOP approach has been widely applied in atmosphere-ocean sciences and achieved significant progress, there are still a few challenges regarding its future use. For example, the model-dependency problem, which cares about the consistency of the CNOPs obtained in different models. Furthermore, the CNOP-based targeted observations for reducing model errors and improving forecasts of climatological mean states also require attention. These challenges have been thoughtfully discussed in Zhang et al. (2020). In addition, with increasing computing power, the implementation of parallel algorithms is in urgent need to save the time cost of calculating the CNOP, which is particularly useful for targeted observations of short-range forecasts. To overcome these difficulties, collaborative efforts from researchers in model development, high-performance computing, numerical forecast, data assimilation and other related fields, are required.

References

[1] Chemin J. Y., Desjardins B., Gallagher I. and Grenier E., An introduction to rotating fluids and the Navier-Stokes equations, Mathematical Geophysics, **32**, The Clarendon Press, Oxford University Press, Oxford, 2006.

[2] Salama, A., Introduction to Geophysical Fluid Dynamics: Physical and Numerical Aspects, 2nd ed., B. Cushman-Roisin and J.-M. Beckers, Academic Press, 2013.

[3] Charney, J. G., FjÖrtoft, R. and Neumann, J. Von, Numerical integration of the barotropic vorticity equation, *Tellus*, **2**, 1950, 237–254.

[4] Bryan, K., A numerical method for the study of the circulation of the world ocean, *J. Comput. Phys.*, **4**, 1969, 347–376.

[5] Randall, D. A., Bitz, C. M., Danabasoglu, G., et al., 100 years of earth system model development, *Meteorol. Monogr.*, **59**, 2019, 12.1–12.66.

[6] Palmer, T. N., Shutts, G. J., Hagedorn, R., et al., Representing model uncertainty in weather and climate prediction, *Annu. Rev. Earth Planet. Sci.*, **33**, 2005, 163–193.

[7] Slingo, J. and Palmer, T., Uncertainty in weather and climate prediction, *Philos. Trans. R. Soc. A Math. Phys. Eng. Sci.*, **369**, 2011, 4751–4767.

[8] Mu, M., Duan, W. and Tang, Y. M., The predictability of atmospheric and oceanic motions: Retrospect and prospects, *Sci. China Earth Sci.*, **60**, 2017, 2001–2012.

[9] Mu, M., Duan, W. and Chou, J., Recent advances in predictability studies in China (1999–2002), *Adv. Atmos. Sci.*, **21**, 2004, 437–443.

[10] Latif, M., Collins, M., Pohlmann, H. and Keenlyside, N., A review of predictability studies of Atlantic sector climate on decadal time scales, *J. Clim.*, **19**, 2006, 5971–5987.

[11] Tang, Y., Zhang, R., Liu, T., et al., Progress in ENSO prediction and predictability study, *Natl. Sci. Rev.*, **5**, 2018, 826–839.

[12] Mu, M. and Wang, Q., Applications of nonlinear optimization approach to atmospheric and oceanic sciences, *Sci. Sin. Math.*, **47**, 2017, 1207–1222.

[13] Thompson, P. D., Uncertainty of initial state as a factor in the predictability of large scale atmospheric flow patterns, *Tellus*, **9**, 1957, 275–295.

[14] Boer, G. J., A study of atmosphere-ocean predictability on long time scales, *Clim. Dyn.*, **16**, 2000, 469–477.

[15] Schneider, T. and Griffies, S. M., A conceptual framework for predictability studies, *J. Clim.*, **12**, 1999, 3133–3155.

[16] Palmer, T. N., Gelaro, R., Barkmeijer, J. and Buizza, R., Singular vectors, metrics, and adaptive observations, *J. Atmos. Sci.*, **55**, 1998, 633–653.

[17] Palmer, T. N. and Zanna, L., Singular vectors, predictability and ensemble forecasting for weather and climate, *J. Phys. A Math. Theor.*, **46**, 2013, 254018.

[18] Lorenz, E. N., A study of the predictability of a 28-variable atmospheric model, *Tellus*, **17**, 1965, 321–333.

[19] Farrell, B. F., Small error dynamics and the predictability of atmospheric flows, *J. Atmos. Sci.*, **47**, 1990, 2409–2416.

[20] Fujii, Y., Tsujino, H., Usui, N., et al., Application of singular vector analysis to the Kuroshio large meander, *J. Geophys. Res. Ocean.*, **113**, 2008.

[21] Zanna, L., Heimbach, P., Moore, A. M. and Tziperman, E., Upper-ocean singular vectors of the North Atlantic climate with implications for linear predictability and variability, *Q. J. R. Meteorol. Soc.*, **138**, 2012, 500–513.

[22] Wang, Q., Mu, M. and Dijkstra, H. A., Effects of nonlinear physical processes on optimal error growth in predictability experiments of the Kuroshio Large Meander, *J. Geophys. Res. Ocean.*, **118**, 2013, 6425–6436.

[23] Geng, Y., Wang, Q., Mu, M. and Zhang, K., Predictability and error growth dynamics of the Kuroshio Extension state transition process in an eddy-resolving regional ocean model, *Ocean Model.*, **153**, 2020, 101659.

[24] Mu, M., Duan, W. and Wang, B., Conditional nonlinear optimal perturbation and its applications, *Nonlinear Process. Geophys.*, **10**, 2003, 493–501.

[25] Cherubini, S., De Palma, P., Robinet, J. C. and Bottaro, A., Rapid path to transition via nonlinear localized optimal perturbations in a boundary-layer flow, *Phys. Rev. E - Stat. Nonlinear, Soft Matter Phys.*, **82**, 2010, 66302.

[26] Pringle, C. C. T. and Kerswell, R. R., Using nonlinear transient growth to construct the minimal seed for shear flow turbulence, *Phys. Rev. Lett.*, **105**, 2010, 154502.

[27] Mu, M., Duan, W., Chen, D. and Yu, W., Target observations for improving initialization of high-impact ocean-atmospheric environmental events forecasting, *Natl. Sci. Rev.*, **2**, 2015, 226–236.

[28] Mu, M., Methods, current status, and prospect of targeted observation, *Sci. China Earth Sci.*, **56**, 2013, 1997–2005.

[29] Mu, M., Duan, W., Wang, Q. and Zhang, R., An extension of conditional nonlinear optimal perturbation approach and its applications, *Nonlinear Process. Geophys.*, **17**, 2010, 211–220.

[30] Duan, W. and Zhou, F., Non-linear forcing singular vector of a two-dimensional quasi-geostrophic model, *Tellus, Ser. A Dyn. Meteorol. Oceanogr.*, **65**, 2013, 18452.

[31] Wang, Q. and Mu, M., A new application of conditional nonlinear optimal perturbation approach to boundary condition uncertainty, *J. Geophys. Res. Ocean.*, **120**, 2015, 7979–7996.

[32] Mu, M., Sun, L. and Dijkstra, H. A., The sensitivity and stability of the oceans thermohaline circulation to finite-amplitude perturbations, *J. Phys. Oceanogr.*, **34**, 2004, 2305–2315.

[33] Zu, Z., Mu, M. and Dijkstra, H. A., Optimal initial excitations of decadal modification of the Atlantic meridional overturning circulation under the prescribed heat and freshwater flux boundary conditions, *J. Phys. Oceanogr.*, **46**, 2016, 2029–2047.

[34] Duan, W., Liu, X., Zhu, K. and Mu, M., Exploring the initial errors that cause a significant "spring predictability barrier" for El Niño events, *J. Geophys. Res. Ocean.*, **114**, 2009, C04022.

[35] Duan, W. and Mu, M., Investigating decadal variability of El Nino-Southern Oscillation asymmetry by conditional nonlinear optimal perturbation, *J. Geophys. Res. Ocean.*, **111**(C7), 2006, C07015.

[36] Mu, M., Yu, Y., Xu, H. and Gong, T., Similarities between optimal precursors for ENSO events and optimally growing initial errors in El Niño predictions, *Theor. Appl. Climatol.*, **115**, 2014, 461–469.

[37] Hu, J. and Duan, W., Relationship between optimal precursory disturbances and optimally growing initial errors associated with ENSO events: Implications to target observations for ENSO prediction, *J. Geophys. Res. Ocean.*, **121**, 2016, 2901–2917.

[38] Mu, M., Xu, H. and Duan, W., A kind of initial errors related to "spring predictability barrier" for El Niño events in Zebiak-Cane model, *Geophys. Res. Lett.*, **34**, 2007, L03709.

[39] van Scheltinga, A. D. and Dijkstra, H. A., Conditional nonlinear optimal perturbations of the double-gyre ocean circulation, *Nonlinear Process. Geophys.*, **15**(5), 2008, 727–734.

[40] Mu, M. and Jiang, Z., A method to find perturbations that trigger blocking onset: Conditional nonlinear optimal perturbations, *J. Atmos. Sci.*, **65**, 2008, 3935–3946.

[41] Jiang, Z. and Wang, D., A study on precursors to blocking anomalies in climatological flows by using conditional nonlinear optimal perturbations, *Q. J. R. Meteorol. Soc.*, **136**, 2010, 1170–1180.

[42] Qin, X. and Mu, M., Influence of conditional nonlinear optimal perturbations sensitivity on typhoon track forecasts, *Q. J. R. Meteorol. Soc.*, **138**, 2012, 185–197.

[43] Wang, Q., Mu, M. and Dijkstra, H. A., The similarity between optimal precursor and optimally growing initial error in prediction of Kuroshio large meander and its application to targeted observation, *J. Geophys. Res. Ocean.*, **118**, 2013, 869–884.

[44] Zhang, K., Wang, Q., Mu, M. and Liang, P., Effects of optimal initial errors on predicting the seasonal reduction of the upstream Kuroshio transport, *Deep. Res. Part I Oceanogr. Res. Pap.*, **116**, 2016, 220–235.

[45] Qin, X. and Mu, M., A study on the reduction of forecast error variance by three adaptive observation approaches for tropical cyclone prediction, *Mon. Weather Rev.*, **139**, 2011, 2218–2232.

[46] Mu, M., Zhou, F. and Wang, H., A method for identifying the sensitive areas in targeted observations for tropical cyclone prediction: Conditional nonlinear optimal perturbation, *Mon. Weather Rev.*, **137**, 2009, 1623–1639.

[47] Zhang, K., Mu, M. and Wang, Q., Identifying the sensitive area in adaptive observation for predicting the upstream Kuroshio transport variation in a 3-D ocean model, *Sci. China Earth Sci.*, **60**, 2017, 866–875.

[48] Mu, M. and Jiang, Z., A new approach to the generation of initial perturbations for ensemble prediction: Conditional nonlinear optimal perturbation, *Chinese Sci. Bull.*, **53**, 2008, 2062–2068.

[49] Jiang, Z. and Mu, M., A comparison study of the methods of conditional nonlinear optimal perturbations and singular vectors in ensemble prediction, *Adv. Atmos. Sci.*, **26**, 2009, 465–470.

[50] Huo, Z., Duan, W. and Zhou, F., Ensemble forecasts of tropical cyclone track with orthogonal conditional nonlinear optimal perturbations, *Adv. Atmos. Sci.*, **36**, 2019, 231–247.

[51] Sun, G. and Mu, M., Response of a grassland ecosystem to climate change in a theoretical model, *Advances in Atmospheric Sciences,* **28**(6), 1266–1278.

[52] Wang, B. and Huo, Z., Extended application of the conditional nonlinear optimal parameter perturbation method in the common land model, *Adv. Atmos. Sci.*, **30**, 2013, 1213–1223.

[53] Sun, G. and Mu, M., A flexible method to determine the sensitive physical parameter combination for soil carbon under five plant types, *Ecosphere*, **8**, 2017, e01920.

[54] Gao, Y., Mu, M. and Zhang, K., Impacts of parameter uncertainties on deep chlorophyll maximum simulation revealed by the CNOP-P approach, *J. Oceanol. Limnol.*, **38**, 2020, 1382–1393.

[55] Duan, W. and Zhao, P., Revealing the most disturbing tendency error of Zebiak-Cane model associated with El Niño predictions by nonlinear forcing singular vector approach, *Clim. Dyn.*, **44**, 2015, 2351–2367.

[56] Mu, M. and Duan W., Applications of conditional nonlinear optimal perturbation to the studies of predictability problems, *Chinese Journal of Atmospheric Sciences*, **37** (2), 2013, 281–296 (in Chinese).

[57] Wang, Q., Mu, M. and Sun, G., A useful approach to sensitivity and predictability studies in geophysical fluid dynamics: Conditional non-linear optimal perturbation, *Natl. Sci. Rev.*, **7**, 2020, 214–223.

[58] Mu, B., Ren, J. and Yuan, S., An efficient approach based on the gradient definition for solving conditional nonlinear optimal perturbation, *Math. Probl. Eng.*, **PT.11**, 2017, 3208431.1–3208431.10.

[59] Wang, B. and Tan, X., A fast algorithm for solving CNOP and associated target observation tests, *Acta Meteorologica Sinica*, **23**, 2009, 387–402.

[60] Wang, B. and Tan, X., Conditional nonlinear optimal perturbations: Adjoint-free calculation method and preliminary test, *Mon. Weather Rev.*, **138**, 2010, 1043–1049.

[61] Zheng, Q., Dai, Y., Zhang, L., et al., On the application of a genetic algorithm to the predictability problems involving "On-Off" switches, *Adv. Atmos. Sci.*, **29**, 2012, 422–434.

[62] Sun, G. and Mu, M., Understanding variations and seasonal characteristics of net primary production under two types of climate change scenarios in China using the LPJ model, *Clim. Change*, **120**, 2013, 755–769.

[63] Chen, L., Duan, W. and Xu, H., A SVD-based ensemble projection algorithm for calculating the conditional nonlinear optimal perturbation, *Sci. China Earth Sci.*, **58**, 2015, 385–394.

[64] Yuan, S., Li, M., Wang, Q., et al., Optimal precursors of double-gyre regime transitions with an adjoint-free method, *J. Oceanol. Limnol.*, **37**, 2019, 1137–1153.

[65] Mu, B., Ren, J., Yuan, S. and Zhou, F., Identifying typhoon targeted observations sensitive areas using the gradient definition based method, *Asia-Pacific J. Atmos. Sci.*, **55**, 2019, 195–207.

[66] Mu, B., Ren, J., Yuan, S. et al., The optimal precursors for ENSO events depicted using the gradient-definition-based method in an intermediate coupled model, *Adv. Atmos. Sci.*, **36**, 2019, 1381–1392.

[67] Ma, X., Mu, M., Dai, G., et al., Influence of arctic sea ice concentration on extended-range prediction of strong and long-lasting ural blocking events in winter, *J. Geophys. Res. Atmo.*, **127**, 2022, e20215D036282.

[68] Yang, Z., Fang, X. and Mu, M., The optimal precursor of El Niño in the GFDL CM2p1 model, *J. Geophys. Res. Ocean.*, **125**, 2020, e2019JC015797.

[69] Zhang, K., Mu, M., Wang, Q., et al., CNOP-based adaptive observation network designed for improving upstream kuroshio transport prediction, *J. Geophys. Res. Ocean.*, **124**, 2019, 4350–4364.

[70] Liang, P., Mu, M., Wang, Q. and Yang, L., Optimal precursors triggering the Kuroshio intrusion into the south china sea obtained by the conditional nonlinear optimal perturbation approach, *J. Geophys. Res. Ocean.*, **34**(6), 2017, 15.

[71] Liu, X., Wang, Q. and Mu, M., Optimal initial error growth in the prediction of the kuroshio large meander based on a high-resolution regional ocean model, *Adv. Atmos. Sci.*, **35**, 2018, 1362–1371.

[72] Zhou, L., Wang, Q., Mu, M. and Zhang, K., Optimal precursors triggering sudden shifts in the antarctic circumpolar current transport through drake passage, *J. Geophys. Res. Ocean.*, **126**, 2021, e2021JC017899.

[73] Zhang, K., Mu, M. and Wang, Q., Increasingly important role of numerical modeling in oceanic observation design strategy: A review, *Sci. China Earth Sci.*, **63**, 2020, 1678–1690.

[74] Liu, K., Guo, W., Da, L., et al., Improving the thermal structure predictions in the Yellow Sea by conducting targeted observations in the CNOP-identified sensitive areas, *Sci. Rep.*, **11**, 2021, 1–14.

[75] Xu, H., Chen, L. and Duan, W., Optimally growing initial errors of El Niño events in the CESM, *Clim. Dyn.*, **56**, 2021, 3797–3815.

[76] Zhou, Q., Chen, L., Duan, W., et al., Using conditional nonlinear optimal perturbation to generate initial perturbations in ENSO ensemble forecasts, *Weather Forecast.*, **36**, 2021, 2101–2111.

[77] Zhou, Q., Duan, W. and Hu, J., Exploring sensitive area in the tropical indian ocean for El Niño prediction: Implication for targeted observation, *J. Oceanol. Limnol.*, **38**, 2020, 1602–1615.

[78] Wei, Y., Mu, M., Ren, H. and Fu, J., Conditional nonlinear optimal perturbations of moisture triggering primary MJO initiation, *Geophys. Res. Lett.*, **46**, 2019, 3492–3501.

[79] Chen, G., Wang, B. and Liu, J., Study on the sensitivity of initial perturbations to the development of a vortex observed in southwest china, *J. Geophys. Res. Atmos.*, **126**, 2021, 1–19.

[80] Peng, F., Mu, M. and Sun, G., Evaluations of uncertainty and sensitivity in soil moisture modeling on the Tibetan Plateau, *Tellus A Dyn. Meteorol. Oceanogr.*, **72**, 2020, 1–16.

[81] Sun, G. and Mu, M., Impacts of two types of errors on the predictability of terrestrial carbon cycle, *Ecosphere*, **12**, 2021, e03315.

[82] Sun, G., Peng, F. and Mu, M., Application of targeted observation in a model's physical parameters for the simulation and forecast of heat flux with a land surface model, *Meteorol. Appl.*, **27**, 2020, e1883.

[83] Wang, L., Shen, X., Liu, J. and Wang, B., Model uncertainty representation for a convection-allowing ensemble prediction system based on CNOP-P, *Adv. Atmos. Sci.*, **37**, 2020, 817–831.

[84] Duan, W., Zhao, P., Hu, J. and Xu, H., The role of nonlinear forcing singular vector tendency error in causing the spring predictability barrier for ENSO, *J. Meteorol. Res.*, **30**, 2016, 853–866.

[85] Tao, L. and Duan, W., Using a nonlinear forcing singular vector approach to reduce model error effects in ENSO forecasting, *Weather Forecast.*, **34**, 2019, 1321–1342.

[86] Tao, L., Duan, W. and Vannitsem, S., Improving forecasts of El Niño diversity: A nonlinear forcing singular vector approach, *Clim. Dyn.*, **55**, 2020, 739–754.

[87] Takaya, K. and Nakamura, H., Mechanisms of intraseasonal amplification of the cold Siberian high, *J. Atmos. Sci.*, **62**, 2005, 4423–4440.

[88] Ding, Y. and Krishnamurti, T. N., Heat budget of the siberian high and the winter monsoon, *Mon. Weather Rev.*, **115**, 1987, 2428–2449.

[89] Luo, D., Chen, X., Dai, A. and Simmonds, I., Changes in atmospheric blocking circulations linked with winter Arctic warming: A new perspective, *J. Clim.*, **31**, 2018, 7661–7678.